3-Nitrotyrosine Modification of SERCA2a in the Aging Heart: A Distinct Signature of the Cellular Redox Environment[†]

Tatyana V. Knyushko,[‡] Victor S. Sharov,[§] Todd D. Williams,[||] Christian Schöneich,[§] and Diana J. Bigelow*,[‡]

Cell Biology and Biochemistry Group, Biological Sciences Division, Pacific Northwest National Laboratory, Richland, Washington 99352, Department of Pharmaceutical Chemistry, University of Kansas, Lawrence, Kansas 66045, Mass Spectrometry Laboratory, University of Kansas, Lawrence, Kansas 66045

Received June 26, 2005; Revised Manuscript Received July 25, 2005

ABSTRACT: In the aging heart, decreased rates of calcium transport mediated by the SERCA2a isoform of the sarcoplasmic reticulum (SR) Ca-ATPase are responsible for the slower sequestration of cytosolic calcium and consequent prolonged muscle relaxation times. We report a 60% decrease in Ca-ATPase activity in the senescent Fischer 344 rat heart relative to that of young adult hearts; this functional decrease can be attributed, in part, to the 18% lower abundance of SERCA2a protein. Here, we show that the additional loss of activity is a result of increased 3-nitrotyrosine modification of the Ca-ATPase. Age-dependent increases in nitration of cardiac SERCA2a are identified using multiple analytical methods. In the young (adult) heart 1 molar equivalent of nitrotyrosine is distributed over at least five tyrosines within the Ca-ATPase, identified as Tyr^{122}, Tyr^{130}, Tyr^{497}, Tyr^{586}, and Tyr^{990}. In the senescent heart, the stoichiometry of nitration increases by more than two nitrotyrosines per Ca-ATPase, coinciding with the appearance of nitrated Tyr^{294}, Tyr^{295}, and Tyr^{753}. The abundant recovery of native analogues for each of the nitrated peptides indicates partial modification of multiple tyrosines within cardiac SERCA2a. In contrast, within skeletal muscle SERCA2a, a homogeneous pattern of nitration appears, with full site (1 mol/mol) nitration of Tyr^{753}, in young, with additional nitration of Tyr^{294} and Tyr^{295}, in senescent muscle. The nitration of these latter vicinal sites correlates with diminished transport function in both striated muscle types, suggesting that these sites provide a mechanism for downregulation of ATP utilization by the Ca-ATPase under conditions of nitrative stress.

Increases in 3-nitrotyrosine-modified (nitrated) forms of proteins have been observed in over 80 different pathologies in a variety of tissues (*1*). Normal aging of skeletal muscle is also associated with increased nitration; in particular, specific nitration of the SERCA2a isoform of the sarcoplasmic reticulum (SR)[1] Ca-ATPase, expressed in slow twitch muscle, is observed (*2*). This modification occurs at stoichiometric levels, increasing from 1.0 ± 0.5 (in young adults) to 3.5 ± 0.7 (in senescent) mol of nitrotyrosine/mol of SERCA2a, and correlates with a 40% loss in Ca-ATPase activity. The absence of other amino acid modifications or changes in protein abundance with age suggests a causal relationship between nitration and loss of function. *In vitro* studies also demonstrate that SERCA2a is inherently sensitive to tyrosine nitration with concomitant functional deficits (*2*). Because the physiological role of the Ca-ATPase is to mediate muscle relaxation through the rate-limiting sequestration of cytosolic calcium after each contractile event, the consequence of nitration-induced inhibition of SERCA2a is the prolonged calcium transient and muscle relaxation observed in senescent skeletal muscle (*3*, *4*).

The appearance of nitrotyrosine in muscle, is a signature of nitric oxide-derived oxidation products such as NO_2, peroxynitrite ($ONOO^-$), or its CO_2 adduct (*5*−*7*). The presence in muscle of peroxynitrite, formed by combination of nitric oxide ($NO^{\cdot}$) and superoxide ($O_2^{\cdot -}$), is consistent with the abundant presence of nitric oxide synthase (NOS) and a high rate of oxidative metabolism producing superoxide in contracting muscle (*8*, *9*). While cellular localization of peroxynitrite generation has not been defined, endothelial and neuronal isoforms of NOS (isoforms 1 and 3) are present

[†] This work was supported by grants from the National Institutes of Health (AG18013 and AG12993).

* To whom correspondence should be addressed: Cell Biology and Biochemistry Group, Pacific Northwest National Laboratory, P.O. Box 999, MS P7-56, Richland, WA 99352. Telephone: (509) 376-2378. Fax: (509) 376-6767. E-mail: diana.bigelow@pnl.gov.

[‡] Pacific Northwest National Laboratory.

[§] Department of Pharmaceutical Chemistry, University of Kansas.

[||] Mass Spectrometry Laboratory, University of Kansas.

[1] Abbreviations: amu, atomic mass unit; ATP, adenosine 5′-triphosphate; BPI, base peak ion; cAMP, adenosine 3′:5′-cyclic monophosphate; BSA, bovine serum albumin; $C_{12}E_9$, polyoxyethylene 9 laury ether; CID, collision-induced dissociation; DTPA, diethylenetriaminepentaacetic acid; DTT, dithiotreitol; EGTA, ethylene glycol-bis(β-aminoethyl ether)-*N*,*N*,*N*′,*N*′-tetraacetic acid; ESI, electrospray ionization; HPLC, high-performance liquid chromatography; IEF, iso-electric focusing; IP, immunoprecipitation; LPS, lipopolysaccharide; MALDI, matrix-assisted laser desorption−ionization; MOPS, 3-(*N*-morpholino) propane sulfonic acid; MS, mass spectrometry; MS/MS, tandem mass spectrometry; NOS, nitric oxide synthase; SDS−PAGE, sodium dodecyl sulfate−polyacrylamide gel electrophoresis; SERCA, sarco/endoplasmic reticulum Ca-ATPase, SR, sarcoplasmic reticulum; TCEP, Tris(2-carboxyethyl) phosphine hydrochloride; TFA, trifluoroacetic acid; Thioglo-1, naphthol-(2,1−6)-pyran-2-carboxylic acid, 10-(2,5-dihydro-2,5-dioxo-*H*-pyrrol-1-yl)-9-methoxy-3-oxo, methyl ester.

10.1021/bi051226n CCC: $30.25
Published on Web 09/02/2005

at the sarcolemma and the SR, respectively; NOS2, induced during inflammation, is more widely distributed within both the cardiac and skeletal myocyte (*10*−*15*). The primary source of superoxide originates as a byproduct of mitochondrial metabolism (*16*). Increased contractile activity in muscle results in increases in both superoxide production and nitric oxide; the latter species is important for enhancing fatigue resistance of contractile fibers.

Nitration of multiple muscle proteins has been observed *in vivo* both as a result of inflammation and with aging; only a few of these have been identified, and little is known regarding the effects of their nitration on myocyte function (*17*, *18*). In addition to aging, increased nitration of SERCA2a has been observed in skeletal muscle undergoing electrical stimulation, in hypercholesteremic aorta, and in ischemic human heart; these results suggest that nitration of SERCA2a represents a marker of unresolved nitrative stress in muscle (*19*−*21*). In view of the high aerobic metabolism of the heart, where approximately one-third of the volume of the cardiomyocyte is comprised of mitochondria, the potential for peroxynitrite formation and SERCA2a nitration would seem greater than that in slow twitch skeletal muscle.

Therefore, we have examined the nitration status of SERCA2a in the heart as a reflection of its redox environment, in particular, in view of the very stable protein half-life (14 days *in vivo*) of the Ca-ATPase (*22*). In the present study, we document the 3-nitrotyrosine modification of SERCA2a in the hearts of Fischer 344 rats, with increased stoichiometries of modification in the aged heart, which correlates with a loss of Ca-ATPase activity. In contrast to the complete modification of selected tyrosines previously observed for SERCA2a in skeletal muscle, the SERCA2a resident in the heart exhibits only partial modification at any given site. This difference suggests a more robust cellular environment for the maintenance of low levels of nitration and functional SERCA2a in the heart as compared with skeletal muscle involving turnover or repair. As in skeletal muscle, the age-related appearance of nitrotyrosines at positions 294 and 295 correlating with the loss of Ca-ATPase activity suggests the functional relevance of these lumenal sites.

EXPERIMENTAL PROCEDURES

Materials. Monoclonal antibody raised against SERCA2a was obtained from Affinity Bioreagents, Inc. (Golden, CO); anti-3-nitrotyrosine monoclonal antibody (clone 1A2-9) was a generous gift of Dr. Joseph Beckman (Linus Pauling Institute, Oregon State University); goat anti-mouse IgG (H + L)-horseradish peroxidase and -alkaline phosphatase conjugates were obtained from Pierce (Rockford, IL). All reagents for gel electrophoresis and immunoblotting were from Bio-Rad (Richmond, CA). Molecular-weight standards including prestained markers were from Gibco BRL (Carlsbad, CA). All other chemicals were analytical-grade or better. The potassium phosphate buffer, imidazole buffer, and sodium bicarbonate buffer employed in the oxidation experiments were treated with 5% (w/v) Chelex-100 (Bio-Rad, Hercules, CA) for 1 h to minimize transition-metal contamination. Wild-type and calmodulin (CaM) mutants, T34C and T34C, 110C were expressed in *Escherichia coli* and purified as previously described (*23*).

Isolation of Cardiac SR. Cardiac SR was isolated as described previously with minor modifications (*24*). Fischer 344 male rats (Harlan Sprague−Dawley, Indianapolis, IN) were sacrificed, and the hearts were removed and placed in ice-cold medium consisting of 25 mM imidazole (pH 7.0), 200 μM phenylmethylsulfonyl fluoride (PMSF), and 10 mM DTT. Alternatively, hearts were frozen in liquid N_2 and stored at −80 °C for later isolation of membranes. All subsequent procedures were done in the cold. The ventricles, trimmed of atria and connective tissue, were minced and homogenized (Silverson L4R homogenizer) in small portions of the same buffer using a total of 15 mL of buffer/mg of ventricle. After centrifugation at $500g_{max}$ for 10 min, the resulting pellet was rehomogenized in the remaining buffer and centrifuged again at $500g_{max}$ for 10 min. Supernatants from both centrifugations were filtered through cheesecloth and centrifuged at $15000g_{max}$ for 10 min. The resulting supernatant was centrifuged at $15000g_{max}$ for 10 min, and this supernatant was centrifuged at $44000g_{max}$ for 30 min. The resulting pellet was resuspended with a small volume of 25 mM imidazole (pH 7.0), 0.6 M KCl, and 10 mM DTT followed by centrifugation at $44000g_{max}$ for 30 min. The resulting pellet was resuspended with a small amount of 25 mM imidazole (pH 7.0), 100 mM KCl, and 10 mM DTT. Protein concentrations were estimated by the BCA Assay (Pierce, Rockford, IL) using bovine serum albumin as the standard.

Immunoprecipitation (IP). Cardiac SR proteins (1 mg/mL final concentration) were solubilized in a buffer consisting of 15 mg/mL $C_{12}E_9$, 10 mM NaH_2PO_4 (pH 7.6), 150 mM NaCl, 10 mM EDTA,, 2 μg/mL aprotinin, 2 μg/mL leupeptin, 1 μg/mL pepstatin, and 200 μM PMSF. After centrifugation for 10 min at $10000g_{max}$ to remove nonsolubilized proteins, the resulting supernatant was divided into two equal parts and incubated overnight at 4 °C with mixing with either monoclonal anti-nitrotyrosine antibody (at a final concentration of 10 μg/mL) or monoclonal anti-SERCA2a antibody (at a final dilution 1:1000). Immune complexes were precipitated for 1.5 h at 4 °C with Protein A Sepharose CL-4B (40 μL of 50% suspension/mL of incubation mixture), washed 3 times with buffer containing 10 mM NaH_2PO_4 (pH 7.6), 150 mM NaCl, 10 mM EDTA, 15 mg/mL $C_{12}E_9$, centrifuged for 15 s at $15000g_{max}$, and resuspended in SDS−PAGE sample buffer (62.5 mM Tris-HCl, 2% SDS, 5% β-mercaptoethanol, 10% glycerol, and 0.001% bromphenol blue).

Amino Acid Analysis. After separation with SDS−PAGE (*25*), proteins were blotted to sequence-grade PVDF membranes and protein bands of interest were cut out, dried, and stored at −20 °C for amino acid analysis. Samples were subjected to acid hydrolysis in 6 N HCl and 1% (w/v) phenol for 20 h at 115 °C. Amino acid extraction from the PVDF membrane and derivatization by phenyl-isothiocyanate (PITC) was performed as previously described with internal amino acid standards (*26*). The calculation of the amino acid composition of the SERCA2a Ca-ATPase was based on an apparent molecular mass of 108 123 Da, not including the molecular mass of 13 Trp and 24 Cys, which are lost during hydrolysis. Nitrotyrosine was quantified on the basis of the area of the peak associated with an authentic nitrotyrosine standard.

Nitration of Cardiac SR Proteins by Peroxynitrite. Peroxynitrite has been synthesized essentially H_2O_2- and nitrite-free by the reaction of ozone with cooled aqueous sodium azide as described previously (*27*), aliquoted, and kept at −70 °C and pH 13 until use. The concentration of stock peroxynitrite was determined by the absorbance ($\epsilon_{302} = 1670$ M^{-1} cm^{-1}) immediately before use. Nitration of SR proteins has been achieved by bolus addition of peroxynitrite stock solution to the protein [5 mg/mL in 25 mM imidazole buffer (pH 7.4) and 25 mM sodium bicarbonate pretreated with Chelex 100] while vortexing. The total volume of added peroxynitrite was no more than 5% of the total volume of the incubation mixture.

Ca^{2+}-Dependent ATPase Activity. Ca^{2+}-dependent ATPase activity was measured at 25 °C by colorimetric determination of inorganic phosphate in the medium of 25 mM MOPS (pH 7.0), 5 mM $MgCl_2$, 0.1 M KCl, 5 mM ATP, 6 μM ionophore, A23187, 112 μM EGTA, and 0.1 mM $CaCl_2$ ($[Ca^{2+}]_{free} = 2$ μM) or in the same medium except without added $CaCl_2$ and 2 mM EGTA ($[Ca^{2+}]_{free} = 3$ nM) as described by Lanzetta et al. (*28*). Determination of calcium-dependent ATPase activity required subtraction of activity assayed in the presence of EGTA (basal activity) from that assayed in the presence of $CaCl_2$ (total ATPase activity).

SDS−PAGE and Western Blotting. SDS−PAGE was performed using 3 or 4% stacking and a 5 or 7.5% separating gel according to the method of Laemmli (*25*). Subsequently, proteins were transferred to a PVDF membrane for 2 h at 100 V on ice using buffer containing 25 mM Tris, 192 mM glycine, and 20% methanol. For detection of the cardiac Ca-ATPase (SERCA2a), blots were probed with anti-SERCA2 monoclonal antibody, clone 2A7-A1 (Affinity Bioreagents, Inc., Golden, CO), with a dilution of 1:10 000. For 3-nitrotyrosine detection, blots were probed with anti-3-nitrotyrosine monoclonal antibody, clone 1A2-9 (a gift of Dr. Joseph Beckman), with a dilution of 1:1000. Anti-mouse secondary antibodies conjugated with alkaline phosphatase or horseradish peroxidase were used.

Reduction of Nitrotyrosine with Dithionite. As a means to confirm the nitrotyrosine modification of protein bands, protein blots were incubated with 1 M dithionite in 0.1 M PBS buffer (pH 9) for 10 min at room temperature prior to incubation with anti-nitrotyrosine; dithionite reduces nitrotyrosine to aminotyrosine. Protein bands that are nitrated and previously had displayed anti-nitrotyrosine antibody binding should exhibit no reaction with anti-nitrotyrosine antibody after dithionite reduction.

ThioGlo-1 Modification of Protein Thiols. For labeling of CaM, thiols were first reduced overnight at room temperature in a solution of 0.4 mg of protein/mL, 50 mM Na phosphate (pH 7.4), and 60 mM SDS (100 μL total volume) with an addition of 250 μL of 50% gel slurry of immobilized TCEP (Pierce, Rockford, IL). CaM was separated from the slurry by low-speed centrifugation (50*g*) for 1 min, estimating the CaM concentration in the supernatant using the extinction coefficient ($\epsilon_{277} = 3029$ M^{-1} cm^{-1}). ThioGlo-1 was added from a stock solution in acetonitrile to this protein solution at a molar ratio of 3 ThioGlo-1/cysteine, incubating for 1 h at 60 °C. Samples were mixed with electrophoresis sample buffer without bromphenol blue or reducing agent and without further sample heating (*29*). For ThioGlo labeling of SERCA2a, 0.04−0.1 mg of cardiac SR protein/mL was subjected to reduction with TCEP prior to labeling with 30 μM ThioGlo-1 under the same conditions as for CaM. The fluorescence of ThioGlo-1 adducts associated with protein bands on SDS−PAGE gels was detected with a Lumi-ImagerF1 (Mannheim Boehringer) equipped with a scanning ultraviolet (UV)-light source (250−450 nm) using the emission filter at 520 nm. A comparison with a ThioGlo-labeled calmodulin mutant having 1 Cys/mol of calmodulin indicated maximal modification of 21 ± 1 mol of free thiols/mol of SERCA2a in cardiac SR.

Two-Dimensional Isolation of SERCA2a for Mass Spectrometry. To isolate nitrated SERCA2a for MS analysis, rat heart SR membranes were subjected to the two-dimensional purification described previously (*30*).

HPLC for ESI−MS. Prior to analysis, all samples were acidified with 4% acetic acid. An Ultra Plus II Micro LC System (Micro Tech Scientific, Sunnyvale, CA) was used for peptide separation. Capillary HPLC was performed on a Zorbax C18SB 300 Å (5 cm × 0.32 mm i.d.) column with a flow rate of 10 μL/min. A nonlinear gradient was used to resolve tryptic peptides (solvent A, 1% MeOH; and solvent B, 99% MeOH in 0.08% aqueous formic acid). The gradient was held at 20% B for 5 min and then ramped to 60% B by 65 min, to 70% B by 75 min, and finally to 95% B by 80 min.

To detect tryptic peptides, a Q-Tof 2 mass spectrometer (Micromass Ltd., Manchester, U.K.) was coupled to the HPLC system. It was operated for maximum resolution with all lenses optimized on the MH_2^{2+} ion from the cyclic peptide Gramicidin S. The cone voltage was 30 eV, and Ar was admitted to the collision cell at a collision energy of 5 eV. Mass spectra were acquired with the time-of-flight analyzer at 11 364 Hz of pusher frequency covering the mass range of 400−3000 amu and accumulating data for 5 s/cycle. Time−mass calibration was made with CsI cluster ions acquired under the same conditions.

Analysis of MS Chromatograms. An exhaustive search for peaks corresponding to nitrated peptides and their native analogues in the MS chromatograms was done using MassLynx 3.5 software (Micromass). The search was performed only for tyrosine-containing peptides assuming that up to two cleavage sites could be missing during the tryptic digest and that methionine sulfoxide could be formed. The retention time of the ions of interest obtained during the first LC−MS run was used for programming further CID experiments in on-line capillary HPLC and nanoflow modes.

ESI MS−MS. Collision-induced dissociation (CID) spectra were acquired by setting the MS1 quadrupole to transmit a precursor mass window of ±1.5 amu. As a collision gas, Ar was admitted at a density that attenuates the beam to 20%, which corresponds to 16 psi on the supply regulator. The collision energy was varied from 20 to 35 eV to obtain a distribution of fragments from low to high mass. Spectra were acquired for 2−5 min at 5 s cycles.

RESULTS

Functional Status of SERCA2a in Aging Heart. Diminished activity of the SR Ca-ATPase in the senescent heart accompanied by decreased levels of both SERCA2 gene transcripts and associated protein has been previously reported (*24*, *31*, *32*). In the present study, we have

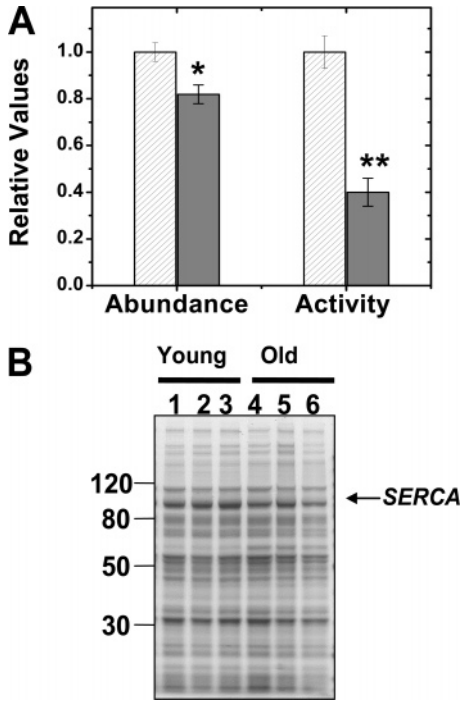

FIGURE 1: Age-related decreases in SERCA2a protein and Ca-ATPase activity in cardiac SR. Relative levels of SERCA2a protein abundance and enzyme activities assessed from measurements of initial rates of calcium-dependent ATP hydrolysis for parallel samples are shown in panel A. SERCA2a protein abundance was estimated from Coomassie Blue-staining of the 110-kDa SERCA2a protein band (indicated in B), identified by its immunoreaction with anti-SERCA2a antibody on Western blots. Bars represent mean values obtained from three separate SR membrane preparations each for young adult (5 month) and senescent (26 month) Fischer 344 rats; each preparation required pooling of 2−3 individual animals, thus utilizing a total of 16 individual (7 young and 9 old) animals. * or ** indicates significant differences in values from senescent hearts relative to those from young hearts of $p < 0.025$ or $p < 0.005$, respectively. Panel B shows Coomassie Blue-stained SDS−PAGE gels of cardiac SR proteins; lanes 1−3 each represent an individual SR preparation isolated from young adult (5 month) rat hearts; lanes 4−6 each represent individual SR preparations isolated from old (26 month) rat hearts. A 4−12% gradient gel was used with MOPS Running buffer (Invitrogen, Carlsbad, CA).

quantitatively compared SERCA2a protein abundance with calcium-dependent ATP hydrolytic rates in SR membranes isolated from the ventricles of 5 month (young adult) and 26 month (senescent) Fischer 344 rats to assess the extent of inhibition of function that is attributable to decreases in the Ca-ATPase protein (Figure 1). Measurements were made from parallel samples of three different SR preparations each from young adult and senescent animals; each preparation resulted from 2 to 3 hearts. Thus, activity and abundance measurements represent data from a total of 16 individuals (7 young and 9 senescent). Ca-ATPase protein levels, estimated from densitometry of the Coomassie Blue-stained 110-kDa protein indicate an 18 ± 1% decrease in the abundance of SERCA2a protein during aging. Corresponding densities from Western blots using anti-SERCA2 antibodies indicate a similar (15 ± 5%) age-related decrease (data not shown). Thus, these complementary methods provide estimates of (i) immunoreactive SERCA2, which may exclude modified forms of SERCA2 and (ii) protein-stained 110-kDa SERCA2, which may include other comigrating proteins. Both methods demonstrate similar decreases in

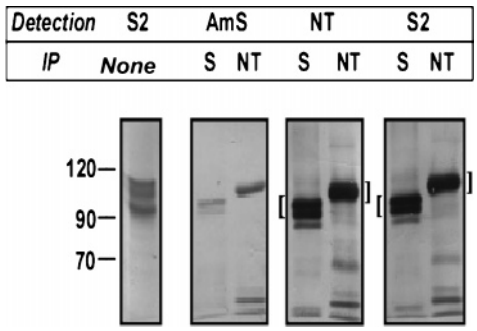

FIGURE 2: IP selects different fractions of nitrated SERCA2a from cardiac SR. Cardiac SR proteins isolated from young adult Fischer 344 rats were solubilized and subjected to IP with anti-SERCA2 (S) antibody or with anti-nitrotyrosine (NT) antibody. Proteins in the resulting IP fractions were separated with 5% SDS−PAGE, blotted onto PVDF membranes, and visualized with Amido Schwartz (AmS) protein stain, anti-SERCA2 antibody (S), or anti-nitrotyrosine (NT) antibody. Previous to IP (indicated as none), cardiac SR proteins were separated on SDS−PAGE and immunoblotted with anti-SERCA2 antibody to indicate the mobility of SERCA2a bands. IP, gels, and blots were performed as described in the Experimental Procedures. Brackets indicate regions on blots that were excised for amino acid analysis (see Table 1).

SERCA2a protein abundance in senescent hearts; this decreased protein abundance is exceeded by the almost 3-fold greater loss of catalytic activity (60 ± 9%). Thus, factors in addition to the rather modest decrease in protein expression are required to explain the functional losses of the Ca-ATPase during aging in the heart.

In Vivo Nitration of SERCA2a in the Heart. The cardiac Ca-ATPase isoform, SERCA2a, normally represents up to 10 wt % of the total SR proteins based on gel densitometry (Figure 1B). To enrich for SERCA2a for analysis, SR proteins were subjected to IP with the primary antibody directed against SERCA2. While this antibody does not discriminate between the alternate splice variants of SERCA2, expression of SERCA2b in the heart is an order of magnitude less than that of SERCA2a (*33*), which typically migrates on SDS−PAGE as a series of protein bands with apparent molecular mass of 95−110 kDa (lane 1 in Figure 2). IP of solubilized SR proteins with a primary antibody specific for SERCA2 isolates a doublet visualized with Amido Schwartz protein stain that migrates with an apparent molecular mass of approximately 90 kDa. An alternate IP of SR, with anti-nitrotyrosine antibody, pulls down a 100-kDa protein band. Thus, the major protein bands immunoprecipitated by nitrotyrosine and SERCA2 antibody, respectively, exhibit the same electrophoretic mobility as higher and lower molecular-weight SERCA2a from SR, further suggesting that antibodies select SERCA fractions with different nitration levels, which, in turn, alter the electrophoretic mobility of SERCA. Somewhat surprisingly, immunoblots show strong intensities related to immunoreaction for both IP products with both anti-SERCA2 and anti-nitrotyrosine antibodies, suggesting that both fractions of SERCA2a are nitrated. The greater sensitivity of immunoblots relative to the Amido Schwartz protein stain provides visualization of additional protein bands corresponding to intact SERCA2a species as well as low molecular-weight fragments of SERCA2a. Confirmation that these IP fractions are nitrated was obtained by amino acid analysis (see below) and in separate experiments in which blotted proteins were

Table 1: Stoichiometry of Nitrotyrosine Modification of SERCA2a Fractions from IP of Cardiac SR[a]

	young		old	
sample	NY/S2	relative yield	NY/S2	relative yield
anti-NY IP	1.7 (±0.3)	0.48	3.8 (±0.3)	0.50
anti-S2 IP	0.2 (±0.1)	0.52	2.4 (±0.3)	0.50
averages	1.0 (±0.5)		3.1 (±0.4)	

[a] SR proteins from young (4−6 month) adult and senescent (26−27 month) Fischer 344 rat hearts were solubilized and immunoprecipitated as described in the Experimental Procedures with either anti-nitrotyrosine (anti-NY) or anti-SERCA2 (anti-S2) antibodies attached to Protein A-Sepharose beads. After separation of the resulting immunoprecipitated proteins on SDS−PAGE and blotting onto sequence-grade PVDF membranes, major protein bands migrating with an apparent molecular mass of 95−110 kDa (as indicated in Figure 2) were excised for amino acid analysis as described previously (*25*). Quantification of nitrotyrosine was based on a peak coeluting with an authentic nitrotyrosine standard. Yields of total protein from each IP ranged from 10 to 20%. The weighted average (average) of the extent of nitration of SERCA2 recovered from young or old cardiac SR was determined on the basis of the relative yields (relative yield) of each IP fraction from densitometry of gel bands.

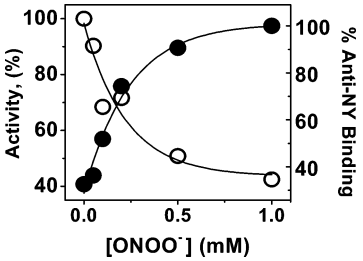

FIGURE 3: Nitration of SERCA2a *in vitro* results in partial inactivation of the Ca-ATPase. SR membranes isolated from young adult hearts of Fischer 344 rats were exposed to up to 1 mM peroxynitrite ($ONOO^-$) by bolus addition to 5 mg of SR protein/mL in 25 mM imidazole (pH 7.4) and 25 mM sodium bicarbonate followed by immediate dilution into Ca-ATPase assay medium or into electrophoresis denaturing buffer. The relative extent of nitration (●) was assessed from densities associated with the SERCA2a by anti-nitrotyrosine immunoblots. Relative Ca-ATPase activity (○) was measured at 25 °C as described in the Experimental Procedures; 100% activity corresponds to 0.15 (±0.01) μmol mg^{-1} min^{-1}. Data represent the average of two different determinations; experimental variability was less than 10% in each case.

treated with dithionite, which reduces nitrotyrosines to aminotyrosines, resulting in the complete loss of subsequent nitrotyrosine antibody binding to the electrophoresed and blotted protein (data not shown).

These nitrated SERCA2a fractions that are selectively isolated by each antibody represent quantitatively distinct fractions; for example, the complete recovery of one IP product results in an immunosupernatant from which the alternate IP product can be fully recovered. It might be hypothesized that the distinct populations of SERCA2a differ in their level of nitrotyrosine modification and can be differentially isolated under the mild detergent concentrations used for IP. In contrast, both antibodies have comparable affinities for all SERCA2a species under the denaturing conditions of Western immunoblots.

Amino acid analysis was performed on the 90−110-kDa protein bands excised from each IP fraction to assess the stoichiometry of nitration based on quantification of a chromatographic peak coeluting with authentic nitrotyrosine (Table 1). The amino acid content also confirmed the identity of the 110-kDa bands as SERCA2a. The anti-nitrotyrosine-derived SERCA2a, which migrates on SDS−PAGE with a higher apparent molecular mass, is more highly nitrated than the anti-SERCA2a IP protein band, suggesting that the basis for the altered electrophoretic mobility of each IP product is differences in post-translational modification. IPs of SR isolated from senescent rat hearts result in similar protein banding patterns but with increased extents of nitration for each fraction, indicating that there is a greater nitration of SERCA2a during aging. The relative yields of SERCA2a IP fractions from young and old hearts are approximately equivalent, suggesting up to a 3-fold increase in nitration of SERCA2a in the aging heart from 1.0 ± 0.2 in young to 3.1 ± 0.3 mol of nitrotyrosine/mol of SERCA2a.

Functional Consequences of Nitration. To test if nitration of SERCA2a results in the loss of activity consistent with the extent of nitration and inactivation in aging, cardiac SR (from young animals) was exposed to varying amounts of peroxynitrite. Progressive increases in nitrotyrosine modification are observed from the appearance of anti-nitrotyrosine immunoblot densities associated with the 110-kDa SERCA2a. This increased nitration correlates with a concomitant loss of calcium-dependent ATP hydrolytic activity saturating at a maximum of 60% inactivation (Figure 3), consistent with previously observed peroxynitrite-induced nitration and inhibition of SERCA2a in skeletal muscle SR (45% inhibition at almost 4 mol of nitrotyrosine/mol of SERCA2a; *2*).

Because peroxynitrite also undergoes rapid rates of reaction with cysteines, the oxidative sensitivity of cysteines within SERCA2a was monitored by the loss of free thiol groups after exposure to peroxynitrite. Free thiols within SERCA2a were assayed by the reaction with ThioGlo-1, a maleimide reagent (naphthol-[2,1-β]pyran-2-carboxylic acid, 10-(2,5-dihydro-2,5-dioxo-*H*-pyrrol-1-yl)-9-methoxy-3-oxo-, methyl ester), which produces a highly fluorescent thiol adduct (Figure 4). The sensitivity of this reagent is illustrated from its labeling of wild-type calmodulin, having no cysteines and no detectable background signal and two mutant calmodulins having one or two cysteines that show proportional increases in fluorescence on reducing SDS−PAGE (lower panel of Figure 4A).

Exposure of SR membranes from young adult hearts to increasing concentrations of peroxynitrite results in a significant loss of ThioGlo-reactive thiols as indicated by the progressive decreases in fluorescence associated with the 110-kDa SERCA2a band on SDS−PAGE (center panel of Figure 4A). This peroxynitrite-induced loss of ThioGlo-reactive free thiols is consistent with irreversible cysteine oxidation, such as sulfinic or sulfonic acid adducts. On the other hand, cardiac SR isolated from young and old rats shows no significant differences in ThioGlo labeling (upper panel of part A and B of Figure 4). Under the denaturing conditions of ThioGlo labeling, approximately 21 ± 1 (of 24 total) cysteines within SERCA2a are modified. Therefore, on the basis of sensitivity of detectable differences in ThioGlo fluorescence of 10%, up to 2 cysteines might be irreversibly modified without detection in this assay. Indeed, a low level (1.5 mol/mol) of cysteine oxidation associated with aging was measured in rat skeletal SR containing a mixture of both SERCA1a and SERCA2a; however, the appearance of this oxidation appears chronologically prior to any loss in Ca-ATPase activity (*26*).

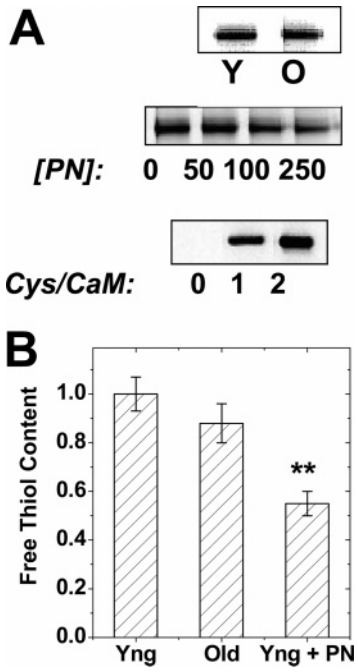

FIGURE 4: Extent of loss of free thiols within SERCA2a from peroxynitrite *in vitro* is not recapitulated *in vivo* with aging. Changes in cysteine oxidation status within SERCA2a were monitored by the loss of thiol reactivity to the fluorescent maleimide reagent, ThioGlo-1 (as described in the Experimental Procedures). A shows the 110-kDa SERCA2a protein on SDS−PAGE after ThioGlo labeling of the following samples: (upper panel) cardiac SR from young adult (Y) and old (O) Fischer 344 rats and (center panel) cardiac SR from young adult rats after exposure to 0, 50, 100, or 250 μM peroxynitrite (PN). A (lower panel) shows ThioGlo-labeled calmodulin species having 0, 1, or 2 cysteines. These calmodulins correspond to the wild type or mutants, Thr110Cys or Thr 34, 110 Cys, respectively. The bar graph in B represents the relative densities of ThioGlo associated with SERCA2a protein from young (Yng), old (Old), and young samples exposed to 250 μM PN (Yng+PN), as an average of three separate determinations for each sample. Error bars represent standard errors. The value of 1.0 represents 21 ± 1 mol of ThioGlo/mol of SERCA2a. Double asterisks (**) indicate a significant difference at $p < 0.05$, relative to the young sample, as determined by Students *t* test.

We further suggest that any cysteine oxidation of SERCA2a in aging heart has minor functional effects compared with tyrosine nitration, as evidenced by the strong correlation between Ca-ATPase inhibition and SERCA2a tyrosine nitration both under *in vivo* (aging) and *in vitro* (peroxynitrite exposure) conditions. In contrast, the extent of cysteine oxidation under *in vitro* or *in vivo* conditions is highly variable, and thus, the correlation with Ca-ATPase activity is poor. Additional insight may be provided by the consideration of the specific cysteine oxidation by peroxynitrite of the homologous isoform, SERCA1, which does not undergo tyrosine nitration; peroxynitrite exposure results in 1.3 mol of cysteine oxidation/mol of SERCA1 with only a 17% decrease in Ca-ATPase activity, attributable to oxidation of Cys^{349} (*50*, *51*).

Sites of Nitrotyrosine Modification with Aging. Sites of tyrosine nitration within cardiac SERCA2a were determined following purification as previously described (*30*). Purification involved an initial separation of SR proteins utilizing a reversed phase (C4) liquid chromatography as the first step, monitoring nitrated protein by the characteristic absorbance at 360 nm of nitrotyrosine at low pH and protein absorbance at 280 nm. This step provides good resolution of several chromatographic peaks enriched in the 110-kDa Ca-ATPase as assessed by SDS−PAGE and avoids alternative methods involving isoelectric focusing, which often provide poor resolution of membrane proteins. SERCA2a was excised and subjected to in-gel digestion; the resulting tryptic peptides were further subjected to reduction and carboxymethylation before their separation by microbore HPLC, in line with a Q-Tof 2 electrospray mass spectrometer. From the resulting mass spectra, searches were performed for peaks corresponding to modified tyrosine-containing peptides and their native analogues. These spectra were interrogated for both nitrotyrosine as well as methionine sulfoxides; the latter modified amino acid might be expected to accompany the former if peroxynitrite is the cellular nitrating agent (*34*). Indeed, as the results show, inclusion of methionine sulfoxide in these searches provides optimal detection of nitrotyrosines because multiple peptides having nitrated tyrosines also contain methionine sulfoxides (Table 2). However, no age-associated increases in methionine-sulfoxide-modified peptides were detected.

From these data, peptides having 10 of the 18 tyrosines within the SERCA2a sequence were identified with sequence coverage, consistent with the overall coverage (66%) of protein sequence previously documented for the homologous SERCA1 isoform. Tyrosine-containing peptides that were not detected represent very long and membrane-spanning sequences, which are resistant to mass spectrometric analysis (*30*). Of the identified peptides, eight have altered elution times with additional masses indicative of nitrotyrosine modification (45 amu/nitration). For each of the modified peptides, their native analogue is also readily detected, indicating that not all Ca-ATPase proteins are modified at a particular tyrosine site. As an example, mass spectra are shown for the nitrated and native peptides $GAIYYFK^{297}$ in young and old samples; the mass 476.3, which corresponds to the nitrated peptide, appears in the old sample but is notably absent in samples from young heart (Figure 5). In young adult hearts, the 1.0 mol of nitrotyrosine/mol of SERCA2a is distributed over at least five tyrosines identified as Tyr^{122}, Tyr^{130}, Tyr^{497}, Tyr^{586}, and Tyr^{990}. In senescent hearts, the same nitrated sites are present with the addition of 2 mol of nitrotyrosine/SERCA2a accompanied by the appearance of 3 nitrated sites, i.e., Tyr^{294}, Tyr^{295}, and Tyr^{753}. While mass spectrometry cannot provide a quantitative description of the relative stoichiometry of each nitrated site, a comparison of the number of sites/mol of total nitrotyrosine would suggest that in young heart SERCA2a has a low extent of nitration at any one site, but more complete nitration of new sites results from aging.

For these age-associated nitrated sites, the corresponding nitrated peptides ($AIY(NO_2)NNMK$ and $GAIY(NO_2)Y(NO_2)FK$ were synthesized for electrospray MS analysis, which resulted in identical masses as those detected from biological samples. Moreover, these same modified peptide masses were identified by MS analysis of the SERCA2 peptide obtained from SR of young heart after PN treatment. From the incomplete recovery of all tyrosine-containing peptides, it cannot be ruled out that additional nitration may occur to these sites that explains the functional effects of aged heart. However, the localization of Tyr^{294} and Tyr^{295} and the potential functional consequences of their nitration are unique and will be discussed.

Table 2: Tyrosine-Containing Peptides in Rat SERCA2a Detected by HPLC−ESI−MS[a]

					cardiac SERCA2a	
Tyr number[b]	peptide sequence[c]	modifications[d]	ion mass computed[e]	ion charge[f]	LC−MS time (min)[g]	ion mass detected[h]
122	EYEPEMGK		491.71	MH_2^{2+}	7−9	491.72
122	EY(NO2)EPEM(O)GK	M(O)	499.71	MH_2^{2+}	7−9	499.73
122	EY(NO2)EPEM(O)GK	Y(NO2), M(O)	522.20	MH_2^{2+}	7−10	522.25
122	NAENAIEALKEYEPEMGK	M(O)	684.66	MH_3^{3+}	64−68	684.68
122	NAENAIEALKEY(NO2)EPEMGK	Y(NO2)	694.32	MH_3^{3+}	50−52	694.32
122	NAENAIEALKEY(NO2)EPEM(O)GK	Y(NO2), M(O)	699.65	MH_3^{3+}	22−27	699.68
122, 130	EYEPEMGKVYR	Y(NO2), M(O)	487.88	MH_3^{3+}	29−31	487.88
122, 130	EY(NO2)EPEM(O)GKVY(NO2)R	Y(NO2), M(O)	731.32	MH_2^{2+}	29−31	731.40
122, 130	EY(NO2)EPEM(O)GKVY(NO2)R	M(O)	708.83	MH_2^{2+}	42−46	708.75
130	VY(NO2)RQDRK	Y(NO2)	505.26	MH_2^{2+}	24−26	505.29
294, 295	GAIYYFK		431.23	MH_2^{2+}	17−20	431.25
294, 295	**GAIY(NO2)Y(NO2)FK***	**2Y(NO2)**	**476.21**	**MH_2^{2+}**	**25−29**	**476.26**
434	GVYEK		595.31	MH^+	10−14	595.33
497	SMSVYCTPNKPSR	C(CM)	509.90	MH_3^{3+}	8−10	509.92
497	SMSVY(NO2)CTPNKPSR	C(CM)	764.35	MH_2^{2+}	8−10	764.37
497	SMSVY(NO2)CTPNKPSRTSM(O)SK	Y(NO2), 2M(O)	694.31	MH_3^{3+}	50−52	694.32
497	SMSVY(NO2)CTPNKPSR	M(O)	743.35	MH_2^{2+}	12−15	743.47
497	KSMSVY(NO2)CTPNKPSR	Y(NO2), C(CM), M(O)	572.93	MH_3^{3+}	30−33	572.97
497	KSMSVY(NO2)CTPNKPSR	Y(NO2), M(O)	829.89	MH_2^{2+}	14−17	829.94
586	YETNLTFVGCVGMLDPPR		671.33	MH_3^{3+}	49−52	671.33
586	Y(NO2)ETNLTFVGCVGM(O)LDPPR	Y(NO2)	686.32	MH_3^{3+}	57−62	686.36
753	AIYNNMK		853.42	MH^+	7−9	853.45
753	**AIY(NO2)NNMK***	**Y(NO2)**	**449.71**	**MH_2^{2+}**	**13−14**	**449.73**
753	AIY(NO2)NNMKQFIR*	Y(NO2), M(O)	486.91	MH_3^{3+}	7−9	486.91
867	VSFYQLSHFLQCK	C(CM)	829.41	MH_2^{2+}	54−57	829.47
990	NYLEPGK	Y(NO2)	433.21	MH_2^{2+}	12−13	433.25
990	NYLEPGK		410.71	MH_2^{2+}	27−32	410.8
990	ISLPVILMDETLKFVARNYLEPGK	Y(NO2), M(O)	702.63	MH_4^{4+}	39−41	702.62

[a] Rat cardiac SERCA2a was purified as described in the Experimental Procedures prior to LC−ESI−MS analysis. Modified peptides and their native analogues containing tyrosine were identified from a search for native peptides and peptides with additional ion masses corresponding to nitration of tyrosine (+45 amu) and methionine sulfoxide (+16 amu); for peptides containing Cys, the presence of carboxymethylation (+42 amu), resulting from iodacetamide treatment, was accounted for. Modified peptides were assumed to match the theoretical mass with a tolerance better than 100 ppm and have a parent native fragment in the spectrum. Peptides in bold were only observed in aged samples. Undetected were Tyr at positions 389, 407, 427, 762, 836, 842, 867, 894, and 948. [b] Represents number of Tyr site in the SERCA2a sequence (ExPASy−P11507 (SERCA2a isoform). [c] Sequence of identified tyrosine-containing peptide; an asterisk indicates that this peptide was observed only in old rats. [d] Modified amino acids: Y(NO2), nitrotyrosine; M(O), methionine sulfoxide; and C(CM), carboxy-methylated cysteine (modification required for MS sample preparation). [e] The tryptic peptide mass simulated by MS-Digest (ProteinProspector program, http://prospector.ucsf.edu/). [f] Charge of identified or computed ion. [g] Experimentally determined LC peptide retention time (in minutes). [h] Experimentally determined ion mass of peptide.

Of note, the vicinal tyrosines, Tyr^{294} and Tyr^{295}, have also been previously identified in their nitrated form in senescent skeletal muscle (*2*). Moreover, for both heart and skeletal muscle, the peptide (GAIYYFK) containing these vicinal tyrosines is recovered either in its native form or as a doubly nitrated peptide; we have not detected the singly nitrated peptide, suggesting that nitration of these vicinal tyrosines is highly cooperative. Thus, both mass spectrometry of peptides, nitrotyrosine antibodies, and cysteine reactive modification with ThioGlo indicate that nitrotyrosine modification of SERCA2a increases with age in the heart and correlates with decreased Ca-ATPase activity.

DISCUSSION

Summary of Results. We have demonstrated age-related increases in 3-nitrotyrosine modification of SERCA2a in the heart by multiple experimental methods, which include immunoblotting, visible spectroscopy, amino acid analysis, and mass spectrometry (Figures 3 and 5 and Tables 1 and 2). Stoichiometries of nitration determined from immunoprecipitated fractions of nitrated SERCA2a show an increase from 1.0 (±0.5) to 3.1 (±0.4) mol of nitrotyrosine/mol of SERCA2a, indicating that the SR Ca-ATPase is a major target of nitrative stress. In young adult hearts, five nitrated tyrosines have been identified; the abundant detection of unmodified peptide analogous to each nitrated peptide indicates partial nitration of each site. From senescent hearts, an additional 2 mol of nitrotyrosines/mol of SERCA2a is identified; additional peptides nitrated at Tyr^{753} and on the vicinal tyrosines, i.e., Tyr^{294} and Tyr^{295}, are present, suggesting close to stoichiometric modification. Modification of these latter sites during aging coincides with the decreased catalytic activity of SERCA2a. *In vitro* experiments demonstrate a similar functional sensitivity of SERCA2a to peroxynitrite, which results in both tyrosine nitration and loss of free thiols, i.e., cysteine oxidation. This result is consistent with recent work demonstrating the correlated appearance of nitrated tyrosines and irreversibly oxidized cysteine adducts of SERCA2(b) in the aorta (smooth muscle) after exposure to high levels of peroxynitrite or under the pathological conditions of athleroschlerosis (*20*). However, during aging in the heart, increased tyrosine nitration is observed, without detectable increases in cysteine oxidation, suggesting that age-dependent decreases in Ca-ATPase function are the result of the nitration of Tyr^{753}, Tyr^{294}, and Tyr^{295}.

Functional Relevance of Nitration at Tyr^{294} and Tyr^{295}. We have previously identified a different pattern of nitration

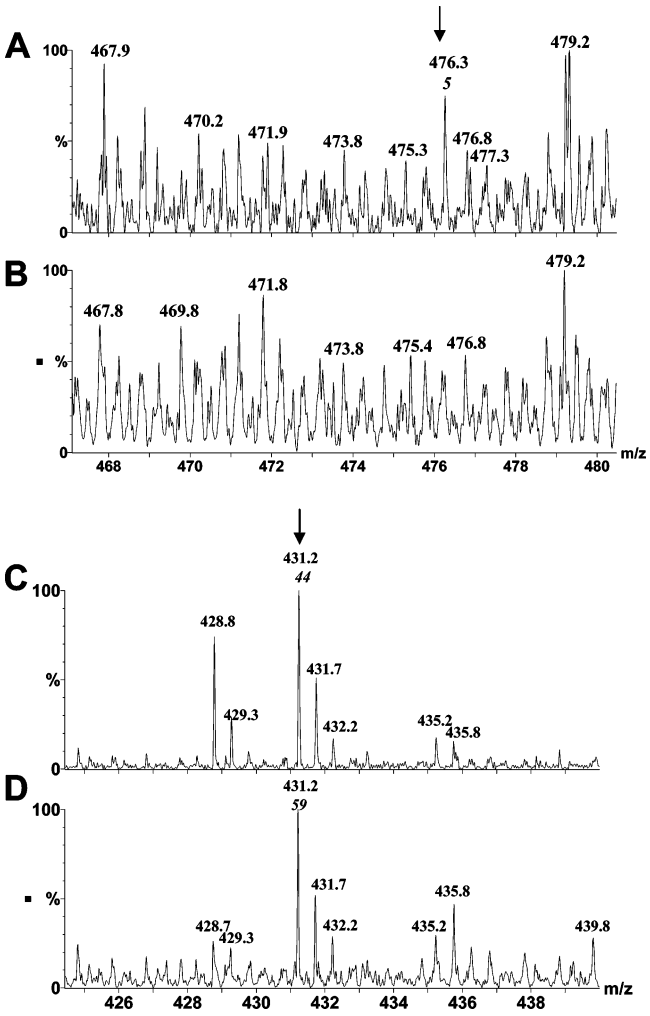

FIGURE 5: Mass spectra of doubly nitrated (A and B) and native (C and D) SERCA2a peptide GAIYYFK[297] from senescent (A and C) and young adult (B and D) heart. Mass spectra in A, indicated by the arrow, show the peak with *m*/*z* 476.3, corresponding to a doubly charged ion of peptide GAIY(NO_2)Y(NO_2)FK; this peak is not detected in the spectra from young heart (B). C and D are mass spectra showing the position of a peak with *m*/*z* 431.2, corresponding to a doubly charged ion of the respective native peptide. Mass spectra were integrated from respective mass chromatograms (25−29 min for A and B, and 17−21 min for C and D). Peaks of interest are indicated by arrows, and their intensities are shown below mass labels.

for SERCA2a in slow twitch skeletal muscle; i.e., a limited number of sites are fully nitrated. Specifically, Tyr^{753} is nitrated in young adult skeletal muscle; 2 additional mol of nitrotyrosine at Tyr^{294} and Tyr^{295} appear in senescent skeletal muscle (Table 3). The common appearance of nitration at Tyr^{294} and Tyr^{295} in both senescent heart and skeletal muscle, correlated with the loss in function, suggests that these vicinal tyrosines play a critical role in the age-related decrease in rates of active calcium transport across the SR. Nitration of Tyr^{753} may have less functional consequences, as suggested by the observation that mutation of this site does not alter Ca-ATPase activity (*35*).

Additional functional effects on SERCA2 may include peroxynitrite-induced modifications of cysteines. A recent study demonstrated that up to 3 mol of cysteines in SERCA2a from heart and in SERCA2b in aortic smooth muscle is glutathiolated by exposure to low levels (10−100 μM) of peroxynitrite in the presence of glutathione. Glutathiolation of Cys^{674}, in particular, correlated with a 25−35% elevation in Ca-ATPase activity (*20*). These glutathione adducts are likely formed through a reversible cysteine oxidation intermediate, e.g., a thiyl radical ($RS^{\cdot}$); at higher peroxynitrite concentrations, glutathiolation of these cysteines is prevented by the formation of irreversible oxidation products (sulfonic acid), accompanied by tyrosine nitration and decreased Ca-ATPase activity. Thus, low levels of peroxynitrite can act in cellular signaling, in this case, as an intermediate between endothelium-derived nitric oxide and activation of smooth muscle relaxation in the aorta, while higher levels of peroxynitrite produce the oxidative modifications of SERCA characteristic of atheroschlerosis. Similarly, the increased nitration of SERCA2a in aging heart suggests the presence of sufficient cellular peroxynitrite to preclude glutathiolation and activation of SERCA2.

Table 3: Summary of Nitrated Tyrosine Sites[a] within SERCA2a: Comparison of Heart with Skeletal Muscle during Aging

young adult		senescent	
skeletal	heart	skeletal	heart
	122		122
	130		130
		294	294
		295	295
	497		497
	586		586
753		753	753
	990		990

[a] Tyrosines within the SERCA2a sequence that have been identified from mass spectrometric analyses as nitrated in heart (Table 2) and skeletal muscle (*2*) in young adult (5 month) and senescent (26−28 month) Fischer 344 inbred rats.

Mechanism of Inhibition. Functional inhibition resulting from nitration of Tyr^{294} and Tyr^{295} can be rationalized by considering the location of these vicinal tyrosines within a functionally critical region of the Ca-ATPase, available from the homologous SERCA1 crystal structure (*36*−*38*). SERCA1 and SERCA2a isoforms are highly homologous with 84% sequence identity and 16 of 18 tyrosine sites in common. Tyr^{294} and Tyr^{295} are located at the lumenal end of the membrane-spanning helix, M4, which is collinear with the enzyme phosphorylation site (Asp^{351}) within the cytosolic phosphorylation (P) domain (Figure 6). The M4 helix accommodates 3 of the 8 ligands required for high-affinity calcium binding and thus provides an essential structural component for the long-range coupling of ATP-linked enzyme phosphorylation with calcium transport. A comparison of high-resolution structures corresponding to major conformations of the Ca-ATPase provides a snapshot of the spatial rearrangements that cytoplasmic and membrane domains undergo during the transport cycle. Both M4 and the nearby M5 helix are pivotal in coordinating movements of membrane-spanning helices with respect to one another (*36*). The dramatic decrease in the pK_a of tyrosine induced by its nitration (from 10 to 7.2) will likely lead to substantial deprotonation of Tyr^{294} and Tyr^{295} occurring in close approximation to the carboxylate group of Glu^{785} (*39*; Figure 7). Thus, the resulting cluster of densely packed negative charges may distort helix−helix interactions at the M4−M5 interface and hinder the coordinated movements of membrane helices that are required for optimal rates of active transport by the Ca-ATPase. Such a proposed mechanism is

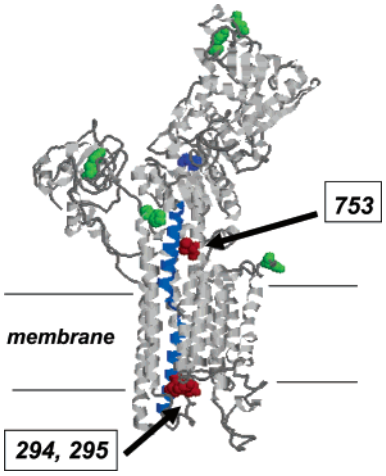

FIGURE 6: Nitrated tyrosine sites within the 3D structure of the Ca-ATPase. Ribbon depiction from the crystal structure of the SERCA1 isoform of the SR Ca-ATPase is shown (PDB code EUL1), indicating, by green (present in young adult or aging heart) or red (present only in aging heart) space-filling depiction, the tyrosines that are nitrated *in vivo*. The M4 helix (Ile^{289}−Lys^{329}) is colored blue; the enzyme phosphorylation site (Asp^{351}) is represented by space-filling depiction in purple.

consistent with the observed partial decrease in the rate of ATPase activity induced by nitration (Figure 2). Of note, Tyr^{294} and Tyr^{295} hold unique positions as the only vicinal tyrosines within the Ca-ATPase polypeptide chain and that are in close proximity to a negatively charged amino acid side chain. Thus, although additional nitrations of other membrane tyrosines that were undetected by this analysis cannot be ruled out, their consequences on helix−helix interactions are unlikely to be of such significance.

Selectivity of Tyrosine Nitration. One of the notable features of SERCA2a nitration is the limited number of the 18 total tyrosines within the SERCA sequence that are nitrated both *in vivo* and *in vitro* (Table 1). This selectivity, also observed for other nitrated proteins, is not fully understood, but several general structural features have been noted for nitrated tyrosines identified within numerous proteins. These features include their location within solvent-accessible loops, at interfaces with lipid bilayers, and the close proximity to a negatively charged side chain; moreover, nitration of transmembrane tyrosines is 10-fold more efficient than in the aqueous phase (*34*, *40*, *41*). Thus, the sensitivities of Tyr^{294} and Tyr^{295} to nitration are consistent with their location both within the membrane and a few angstroms away from the negative charge of the carboxylate group of Glu^{785} as well as the documented ability of peroxynitrite to penetrate bilayers (*42*).

High-resolution structures of the Ca-ATPase crystallized under conditions stabilizing the E1 and E2 conformations highlight the proximity and the altered relative positions of Glu^{785} to Tyr^{294} and Tyr^{295} during the transport cycle (Figure 7). This structural arrangement is consistent with a high probability of nitration of both tyrosines. In support of this suggestion, in our mass spectrometry analyses, of both skeletal muscle and heart SERCA2a, only native or doubly nitrated GAIYYF peptides are detected; we have not detected the singly nitrated peptide (Table 2 and ref *2*). Thus, the position of these vicinal tyrosines within a functionally critical membrane region of SERCA2a and close to a negatively charged side chain would seem to ensure both efficient nitration and a mechanism for decreased rates of calcium transport.

Multiple Cellular Aspects Determine the Persistence of Tyrosine Nitration In Vivo. Steady-state levels of nitrotyrosine-modified proteins in tissue results from a dynamic balance between multiple aspects of the cellular redox environment. These include the abundance of nitrating species, antioxidant status, and the oxidative sensitivities of protein substrates that determine the initial appearance of nitrated proteins, coupled with efficiencies of cellular pathways that remove modified proteins. Defects in any of these features will result in the accumulation of increased amounts and new sites of modification, as observed by the increased SERCA2a nitration at specific sites in aging heart and skeletal muscle. Thus, *in vitro* experiments exposing isolated proteins to reactive species may better identify the

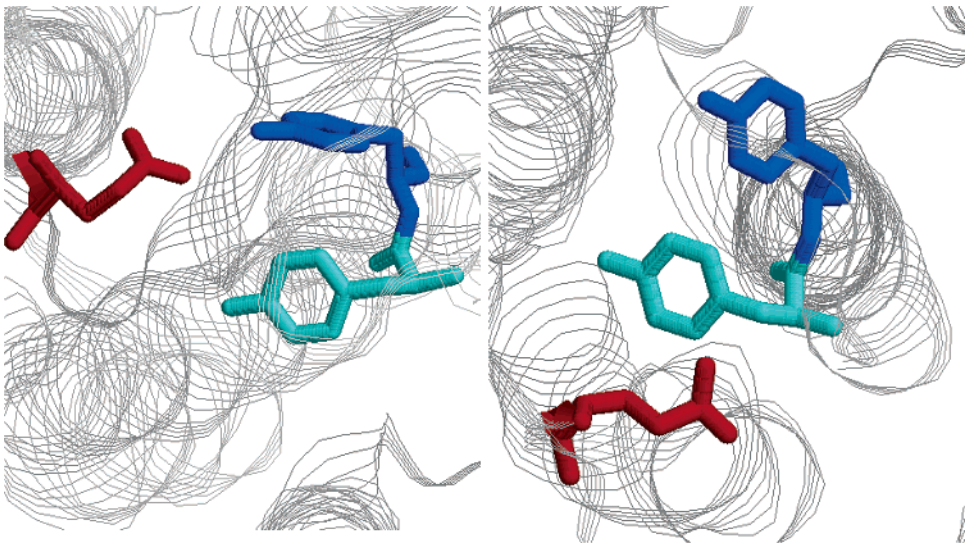

FIGURE 7: Proximity of the negative charge of Glu^{785} to Tyr^{294} and Tyr^{295} within SERCA. The lumenal end of membrane-spanning helices M4 (Ile^{289}−Lys^{329}) and M5 (Asn^{739}−Thr^{778}) is depicted from structures for SERCA1 in the E1−Ca conformation (PDB code 1EUL, left panel) and the E2−thapsigargin conformation (PDB code 1IWO, right panel). The relative proximity of Glu^{785} (red) to Tyr^{294} (aqua) and Tyr^{295} (blue) changes during calcium transport.

sensitivities of pure proteins to oxidation rather than provide a model of the steady-state oxidation products in the cell during aging. For example, Tyr^{122} within the fast twitch skeletal muscle isoform, SERCA1, has been identified as a sensitive site from *in vitro* nitration experiments, but Tyr^{122} has not been detected *in vivo* in skeletal muscle (*30*). Similarly, within SERCA2a, a nitrated peptide containing Tyr^{122} and Tyr^{130} has been identified after mild *in vitro* exposure of skeletal muscle SR to peroxynitrite but is absent in SR isolated from skeletal muscle (*2*).

From a functional standpoint, efficient cellular removal of nitrated Tyr^{122} might be expected as an effective strategy to maintain optimal muscle contractility, because the reversible formation of a hydrogen bond involving this tyrosine is essential in the catalytic cycle of the Ca-ATPase (*36*). The mechanisms involved in removal of nitrated proteins, whether by degradation of the entire protein or enzymatic conversion of the nitrotyrosine to tyrosine, have not been elucidated for the SR Ca-ATPase. Whereas, the 20S proteasome in complex with Hsp90 and independent of ubiquitin and ATP has been demonstrated to degrade oxidized cytosolic proteins; the 10 membrane-spanning sequences of the Ca-ATPase may require alternative or additional degradation proteins (*43*, *44*). A putative denitrase activity identified in tissues and cultured macrophages may represent a more rapid mechanism for maintaining low levels of nitrated proteins (*45*, *46*). Determination of cellular defects in aging will require a more complete understanding of nitration sensitivities of proteins as well as the identification of defects in cellular mechanisms relevant to nitrated SERCA2a.

Physiological Role for SERCA2a Nitration. The appearance of increased nitration and partial inactivation of SERCA2a in several types of muscle under conditions of chronic oxidative stress suggests that a common functional response to nitrative stress of the muscle involves prolongation of the calcium transient with slower contraction and relaxation times of the muscle (*19*−*21*). Such partial inhibition of Ca-ATPase activity when all Ca-ATPase proteins are nitrated suggests a regulatory mechanism rather than pathology. Thus, downregulation of the Ca-ATPase may permit cellular survival from oxidative stress through the conservation of ATP. A decreased need for ATP synthesis will, in turn, minimize superoxide generation in the mitochondria, thus preventing further oxidative damage and facilitate recovery of cellular functions. In particular, in muscle, SERCA represents an effective target for energy conservation because active calcium transport is a major use of ATP required for the restoration of the 10 000-fold calcium ion gradient across the SR membrane after each contractile event. At the same time, the functional link between the Ca-ATPase and contractile rates implies that nitration of SERCA also diminishes ATP utilization by the myosin ATPase. This hypothesis is consistent with the many compensatory changes, both at the molecular and physiological levels, that the aging heart undergoes to maintain function, with the primary role of iNOS in muscle tissue nitration and the elevated levels in aging of iNOS that may produce increased peroxynitrite that maintains SERCA in a nitrated form (*17*, *47*, *48*). Future studies should explicitly address these models and the specific effects of SERCA nitration on myocyte function.

In addition to immediate effects of nitration of SERCA on muscle contractility and energy metabolism, chronic nitration of SERCA may alter patterns of calcium-dependent gene transcription, consistent with processes such as muscle differentiation, skeletal muscle fiber type specification, and cardiac hypertrophy, that are known to result from altered properties of the calcium transient linked to transcriptional activation of genes (*49*).

Conclusions. The broader distribution of nitrated sites and their lower levels of modification of SERCA2a in the heart as compared with skeletal muscle suggest a more robust cellular environment in the heart for maintaining low levels of nitration and optimal function of SERCA in the presence of substantial nitrative stress. Differences between nitration patterns of the same isoform expressed in two different striated muscle types are an indication that pathways for prevention and removal of nitrated proteins also varies. However, the common appearance, in aging of both skeletal muscle and heart, of nitrated Tyr^{294} and Tyr^{295} that correlates with partial inhibition of Ca-ATPase activity suggests that these sites provide a mechanism for the downregulation of ATP utilization by the Ca-ATPase and other linked ATPases under conditions of nitrative stress.

ACKNOWLEDGMENT

We thank Curt Boschek for the gift of purified wild-type and mutant calmodulins and Thomas Squier for helpful discussions.

REFERENCES

1. Ischiropoulos, H. (1998) Biological tyrosine nitration: A pathophysiological function of nitric oxide and reactive oxygen species, *Arch. Biochem. Biophys. 356*, 1−11.
2. Viner, R. I., Ferrington, D. A., Williams, T. D., Bigelow, D. J., and Schoneich, C. (1999) Protein modification during biological aging: Selective tyrosine nitration of the SERCA2a isoform of the sarcoplasmic reticulum Ca-ATPase, *Biochem. J. 340*, 657−659.
3. Toyoshima, C., and Inesi, G (2004) Structural basis of ion pumping by Ca^{2+}-ATPase of the sarcoplasmic reticulum, *Annu. Rev. Biochem. 73*, 269−292.
4. Narayanan, N., Jones, D. L., Xu, A., and Yu, J. C. (1996) Effects of aging on sarcoplasmic reticulum function and contraction duration in skeletal muscles of the rat, *Am. J. Physiol. 271*, C1032−C1040.
5. Beckman, J. S., and Koppenol, W. H. (1996) Nitric oxide, superoxide, and peroxynitrite: The good, the bad, and ugly, *Am. J. Physiol. 271*, C1424−C1437.
6. Tien, M., Berlett, B. S., Levine, R. L., Chock, P. B., and Stadtman, E. R. (1999) Peroxynitrite-mediated modification of proteins at physiological carbon dioxide concnetrations: pH dependence of carbonyl formation, tyrosine nitration, and methionine oxidation, *Proc. Natl. Acad. Sci. U.S.A. 96*, 7809−7814.
7. Reiter, C. D., Teng, R.-J., and Beckman, J. S. (2000) Superoxide reacts with nitric oxide to nitrate tyrosine at physiological pH via peroxynitrite, *J. Biol. Chem. 275*, 32460−32466.
8. Reid, M. B., and Durham, W. J. (2002) Generation of reactive oxygen and nitrogen species in contracting skeletal muscle, *Ann. N.Y. Acad. Sci. 959*, 108−116.
9. Massion, P. B., Feron, O., Dessy, C., and Balligand, J. L. (2003) Nitric oxide and cardiac function: Ten years after, and continuing, *Circ. Res. 93*, 388−398.
10. Boczkowski, J., Lanone, S., Ungureanu-Longrois, D., Danialou, G., Fournier, T., and Aubier, M. (1996) Induction of diaphragmatic nitric oxide synthase after endotoxin administration in rats: role on diaphragmatic contractile dysfunction, *J. Clin. Invest. 98*, 1550−1559.
11. Hussain, S. N., Giaid, A., El Dawiri, Q., Sakkal, D., Hattori, R., and Guo, Y. (1997) Expression of nitric oxide synthases and GTP cyclohydrolase I in the ventilatory and limb muscles during endotoxemia, *Am. J. Respir. Cell Mol. Biol. 17*, 173−180.

12. Xu, K. Y., Huso, D. L., Dawson, T. M., Bredt, D. S., and Becker, L. C. (1999) Nitric oxide synthase in cardiac sarcoplasmic reticulum, *Proc. Natl. Acad. Sci. U.S.A. 96*, 657−662.
13. Afulukwe, I. F., Cohen, R. I., Zeballos, G. A., Iqbal, M., and Scharf, S. M. (2000) Selective NOS inhibition restores myocardial contractility in endotoxemic rates; however, myocardial $NO^{\cdot}$ content does not correlate with myocardial dysfunction, *Am. J. Respir. Crit. Care Med. 162*, 21−26.
14. Buchwalow, I. B., Schulze, W., Karczewski, P., Kostic, M. M., Wallukat, G., Morwinski, R., Krause, E. G., Muller, J., Paul, M., Slezak, J., Luft, F. C., and Haller, B. (2001) Inducible nitric oxide synthase in the myocard, *Mol. Cell. Biochem. 217*, 73−82.
15. Gealekman, O., Abassi, Z., Rubinstein, I., Winaver, J., and Binah, O. (2002) Role of myocardial inducible nitric oxide synthase in contractile dysfunction and β-adrenergic hypo-responsiveness in rats with experimental volume-overload heart failure, *Circulation 105*, 236−243.
16. Cadenas, E. (2004) Mitochondrial free radical production and cell signaling, *Mol. Aspects Med. 25*, 17−26.
17. Barreiro, E., Comtois, A. S., Gea, J., Laubach, V. E., and Hussain, S. N. (2002) Protein tyrosine nitration in the ventilatory muscles: Role of nitric oxide synthases, *Am. J. Respir. Cell Mol. Biol. 26*, 438−446.
18. Kanski, J., Alterman, M. A., and Schoneich, C. (2003) Proteomic identification of age-dependent protein nitration in rat skeletal muscle, *Free Radical Biol. Med. 35*, 1229−1239.
19. Klebl, B. M., Ayoub, A. T., and Pette, D. (1998) Protein oxidation, tyrosine nitration, and inactivation of sarcoplasmic reticulum Ca^{2+}-ATPase in low-frequency stimulated rabbit muscle, *FEBS Lett. 422*, 381−384.
20. Adachi, T., Matsui, R., Xu, S., Kirber, M., Lazar, H. L., Sharov, V. S., Schöneich, C., and Cohen, R. A. (2002) Antioxidant improves smooth muscle sarco/endoplasmic reticulum Ca^{2+}-ATPase function and lowers tyrosine nitration in hypercholesterolemia and improves nitric oxide-induced relaxation, *Circ. Res. 90*, 1114−1121.
21. Lokuta, A. J., Maertz, N. A., Kamp, J. F., Valdivia, H. H., and Haworth, R. A. (2002) Increased tyrosine nitration of SERCA2a in human heart failure inhibits SR Ca-pump function, *Biophys. J. 82*, 597a.
22. Ferrington, D. A., Krainev, A. G., and Bigelow, D. J. (1998) Altered turnover of calcium regulatory proteins of the SR in aged skeletal muscle, *J. Biol. Chem. 273*, 5885−5891.
23. Strasburg, G., Hogan, M., Birmachu, W., Thomas, D. D., and Louis, C. F. (1988) Site-specific derivatives of wheat germ calmodulin: Interactions with troponin and sarcoplasmic reticulum, *J. Biol. Chem. 263*, 542−548.
24. Taffet, G. E., and Tate, C. A. (1992) The MgATPase activity of rat cardiac sarcoplasmic reticulum is a function of the calcium ATPase protein, *Arch. Biochem. Biophys. 299*, 287−294.
25. Laemmli, U. K. (1970) Cleavage of structural proteins during the assembly of the head of bacteriophage T4, *Nature 227*, 680−685.
26. Viner, R. I., Ferrington, D. A., Aced, G. I., Miller-Schlyer, M., Bigelow, D. J., and Schoneich, C. (1997) *In vivo* aging of rat skeletal muscle sarcoplasmic reticulum Ca-ATPase: Chemical analysis and quantitative simulation by exposure to low levels of peroxyl radicals, *Biochim. Biophys. Acta 1329*, 321−335.
27. Pryor, W. A., Cueto, R., Jin, X., Koppenol, W. H., Ngu-Schwemlein, M., Squadrito, G. L., Uppu, P. L., and Uppu, R. M. (1995) A practical method for preparing peroxynitrite solutions of low ionic strength and free of hydrogen peroxide, *Free Radical Biol. Med. 18*, 75−83.
28. Lanzetta, P. A., Alvarez, L. J., Reinach, P. S., and Candia, D. A. (1979) An improved assay for nanomole amounts of inorganic phosphate, *Anal. Biochem. 100*, 95−97.
29. Fabisiak, J. P., Sedlov, A., and Kagan, V. (2002) Quantification of oxidative/nitrosative modification of Cys34 in human serum albumin using a fluorescence-based SDS−PAGE assay, *Antioxid. Redox Signaling 4*, 855−865.
30. Sharov, V. S., Galeva, N. A., Knyushko, T. V., Bigelow, D. J., Williams, T. D., and Schoneich C. (2002) Two-dimensional separation of the membrane protein sarcoplasmic reticulum Ca-ATPase for high-performance liquid chromatography−tandem mass spectrometry analysis of posttranslational protein modifications, *Anal. Biochem. 308*, 328−335.
31. Froehlich, J. P., Lakatta, E. G., Beard, E., Spurgeon, H. A., Weisfeldt, M. L., and Gerstenblith, G. (1978) Studies of sarcoplasmic reticulum function and contraction duration in young adult and aged rat myocardium, *J. Mol. Cell Cardiol. 10*, 427−438.
32. Anisimov, S. V., Tarasov, K. V., Stern, M. D., Lakatta, E. G., and Boheler, K. R. (2002) A quantitative and validated SAGE transcriptome reference for adult mouse heart, *Genomics 80*, 213−222.
33. Wu, K.-D., and Lytton, J. (1993) Molecular cloning and quantification of sarcoplasmic reticulum Ca^{2+}-ATPase isoforms in rat muscle, *Am. J. Physiol. 264 (Cell Physiol. 33)*, C333−C341.
34. Smallwood, H. S., Galeva, N. A., Bartlett, R. K., Urbauer, R. J., Williams, T. D., Urbauer, J. L., and Squier, T. C. (2003) Selective nitration of Tyr99 in calmodulin as a marker of cellular conditions of oxidative stress, *Chem. Res. Toxicol. 16*, 95−102.
35. Sorensen, T. L., and Andersen, J. P. (2002) Importance of stalk segment S5 for intramolecular communication in the sarcoplasmic reticulum Ca^{2+}-ATPase, *J. Biol. Chem. 275*, 28954−28961.
36. Toyoshima, C., and Nomura, H. (2002) Structural changes in the calcium pump accompanying the dissociation of calcium, *Nature 418*, 605−611.
37. Sorenson, T. L.-M., Moeller, J. V., and Nissen, P. (2004) Phosphoryl transfer and calcium ion occlusion in the calcium pump, *Science 304*, 1672−1675.
38. Toyoshima, C., Nakasako, M., Nomura, H., and Ogawa, H. (2000) Crystal structure of the calcium pump of sarcoplasmic reticulum at 2.6 Å resolution, *Nature 405*, 647−655.
39. Creighton, T. E. (1993) *Proteins: Structures and Molecular Properties*, 2nd ed. pp 15−16, W. H. Freeman and Co., New York.
40. Zhang, H., Bhargava, K., Keszler, A., Feix, J., Hogg, N., Joseph, J., and Kalyanaraman, B. (2003) Transmembrane nitration of hydrophobic tyrosyl peptides: Localization, characterization, mechanism of nitration, and biological implications, *J. Biol. Chem. 278*, 8969−6978.
41. Souza, J. M., Daikhin, E., Yudkoff, M., Raman, C. S., and Ischiropoulos, H. (1999) Factors determining the selectivity of protein tyrosine nitration, *Arch. Biochem. Biophys. 371*, 169−178.
42. Marla, S. S., Lee, J., and Groves, J. T. (1997) Peroxynitrite rapidly permeates phospholipid membranes, *Proc. Natl. Acad. Sci. U.S.A. 94*, 14243−14248.
43. Grune, T., Merker, K., Sandig, G., and Davies, K. J. (2003) Selective degradation of oxidatively modified protein substrates by the proteasome, *Biochem. Biophys. Res. Commun. 305*, 709−718.
44. Whittier, J. E., Xiong, Y., Rechsteiner, M. C., and Squier, T. C. (2004) Hsp90 enhances degradation of oxidized calmodulin by the 20S proteasome, *J. Biol. Chem. 279*, 46135−46142.
45. Kamisaki, Y., Wada, K., Bian, K., Balabanli, B., Davis, K., Martin, E., Behbod, F., Lee, Y.-C., and Murad, F. (1998) An activity in rat tissues that modifies nitrotyrosine-containing proteins, *Proc. Natl. Acad. Sci. U.S.A. 95*, 11584−11589.
46. Irie, Y., Saeki, M., Kamisaki, Y., Martin, E., and Murad, F. (2003) Histone H1.2 is a substrate for denitrase, an activity that reduces nitrotyrosine immunoreactivity in proteins, *Proc. Natl. Acad. Sci. U.S.A. 100*, 5634−5639.
47. Lakatta, E. G., and Sollott, S. J. (2002) Perspectives on mammalian cardiovascular aging: Humans to molecules, *Comp. Biochem. Physiol., Part A: Mol. Integr. Physiol. 132*, 699−721.
48. Yang, B., Larson, D. F., and Watson, R. R. (2005) Modulation of iNOS activity in age-related cardiac dysfunction, *Life Sci. 75*, 655−667.
49. Bassel-Duby, R., and Olson, E. N. (2003) Role for calcineurin in striated muscle: Development, adaptation, and disease, *Biochem. Biophys. Res. Commun. 11*, 1133−1141.
50. Viner, R. I., Huhmer, A. F. R., Bigelow, D. J., and Schoneich, C. (1996) The oxidative inactivation of sarcoplasmic reticulum Ca^{2+}-ATPase by peroxynitrite, *Free Radical Res. 24*, 243−259.
51. Viner, R. I., Williams, T. D., and Schoneich, C. (1999) Peroxynitrite modification of protein thiols: Oxidation, nitrosylation, and S-glutathiolation of functionally important cysteine residue(s) in the sarcoplasmic reticulum Ca-ATPase, *Biochemistry 38*, 12408−12415.

BI051226N